

## Quantitative Analysis of Cell Tracing by *in vivo* Imaging System\*

Junmeng ZHENG (郑俊猛)<sup>1†</sup>, Lijun XU (徐利军)<sup>1,2†</sup>, Hongmin ZHOU (周鸿敏)<sup>1,2</sup>, Weina ZHANG (张维娜)<sup>1</sup>,  
Zhonghua CHEN (陈忠华)<sup>1#</sup>

<sup>1</sup>Institute of Organ Transplantation, Key Lab of Ministry of Education/Ministry of Health of China, Tongji Hospital, Tongji Medical College, Huazhong University of Science and Technology, Wuhan 430030, China

<sup>2</sup>Department of Cardiothoracic Surgery, Tongji Hospital, Tongji Medical College, Huazhong University of Science and Technology, Wuhan 430030, China

©Huazhong University of Science and Technology and Springer-Verlag Berlin Heidelberg 2010

**Summary:** *In vivo* imaging system (IVIS) is a new and rapidly expanding technology, which has a wide range of applications in life science such as cell tracing. By counting the number of photons emitted from a specimen, IVIS can quantify biological events such as tumor growth. We used B16F10-luc-G5 tumor cells and 20 Balb/C mice injected subcutaneously with B16F10-luc-G5 tumor cells ( $1 \times 10^6$  in 100  $\mu$ L) to develop a method to quantitatively analyze cells traced by IVIS *in vitro* and *in vivo*, respectively. The results showed a strong correlation between the number of tumor cells and the intensity of bioluminescence signal ( $R^2=0.99$ ) under different exposure conditions in *in vitro* assay. The results derived from the *in vivo* experiments showed that tumor luminescence was observed in all mice by IVIS at all days, and there was significant difference ( $P<0.01$ ) between every two days from day 3 to day 14. Moreover, tumor dynamic morphology could be monitored by IVIS when it was invisible. There was a strong correlation between tumor volume and bioluminescence signal ( $R^2=0.97$ ) by IVIS. In summary, we demonstrated a way to accurately carry out the quantitative analysis of cells using IVIS both *in vitro* and *in vivo*. The data indicate that IVIS can be used as an effective and quantitative method for cell tracing both *in vitro* and *in vivo*.

**Key words:** *in vivo* imaging system; cell tracing; quantitative analysis

*In vivo* imaging system (IVIS) is one of the primary tools used to evaluate structure and function non-invasively in a living subject. Many technologies, including magnetic resonance imaging (MRI), optical imaging, computed tomography (CT), positron emission tomography (PET) and ultrasound, are successfully employed to study the *in vivo* tissues. Among them, the optical imaging based on intrinsic optical properties of tissues is widely used for tracking and reporting functional information on molecules, proteins, and cells *in vivo*. This new technology has been applied to the study of oncology and gene expression in light-producing transgenic cells and small animals through tracing cells of interest. However, while there are studies on qualitative analysis of cells using optical imaging, the quantitative analysis of cells by IVIS has not been reported yet. In this study, we developed simple but accurate assays to quantitatively analyze cells traced by IVIS both *in vitro* and *in vivo*.

Junmeng ZHENG, E-mail: zhengjunmeng@hotmail.com

<sup>†</sup>These authors contributed equally to this work.

<sup>#</sup>Corresponding author, E-mail: zc104@medmail.com.cn

\*This project was supported by a grant from the National Natural Sciences Foundation of China (No. 30901364), and grants from the National Basic Research Program of China (No. 2003CB515505, 2009CB522407).

## 1 MATERIALS AND METHODS

### 1.1 Materials, Main reagents and Equipment

B16F10-luc-G5 cells (mouse melanoma cells labeled with luciferase gene), D-Luciferin Firefly, and potassium salt (light-emitting substrate for fluorescence) were purchased from Xenogen Corporation (USA). Balb/C male mice, weighing 15–20 g and aged 5–7 weeks, were supplied by Animal Center of Institute of Organ Transplantation, Tongji Hospital, Tongji Medical College, Huazhong University of Science and Technology (China). RPMI1640 medium was purchased from Hyclone (USA). The images were collected on an *in vivo* imaging system Lumina 100 from Xenogen Corporation (USA) and fluorescence spectra were recorded on an inverted fluorescence microscope CKX41 from Olympus Corporation (Japan).

### 1.2 Cell Culture

B16F10-luc-G5 cells were grown in RPMI1640 medium supplemented with 100 U/mL of 10% fetal bovine serum, 100 U/mL penicillin/streptomycin, in a humidified atmosphere at 37°C in 5% CO<sub>2</sub>. B16F10-luc-G5 cells were digested by 0.25% trypsin, washed twice with RPMI1640 medium and resuspended at a concentration of  $1 \times 10^5$ /mL cells in the same medium.

### 1.3 *In vitro* Assay

The assay was carried out in 96-well plates. Serial dilutions of the cells in the 96-well plates were prepared

by mixing 100  $\mu\text{L}$  of  $10^5/\text{mL}$  tumor cells with 100  $\mu\text{L}$  of RPMI1640 medium resulting in a 2 fold dilution. 100  $\mu\text{L}$  of the mixture was then pipetted in the well (containing 100  $\mu\text{L}$  1640 medium), mixed, and 100  $\mu\text{L}$  of this mixture was pipetted into the next well, and so on until one had about 8 wells with a decreasing concentration gradient. The number of cells and well number were shown in table 1 and fig. 1, respectively (there were blank intervals between the various wells in order to avoid mutual influence). Bioluminescence detection was conducted by adding 100  $\mu\text{L}$  of 300  $\mu\text{g}/\text{mL}$  D-Luciferin solution (the working concentration was 150  $\mu\text{g}/\text{mL}$ ) to each well for 2—3 min, followed by imaging the plate at exposure time 30 s, 60 s, 180 s, 360 s, 600 s under the preset condition of 10 bin (bin for binning, meaning sensitivity) and FOV12.5 (FOV for field of view, meaning distance between object and camera lens). Quantitative analysis was achieved by analyzing the correlation between the number of tumor cells and the intensity of the bioluminescence.

#### 1.4 In vivo Experiments

To establish the model of inoculated tumor, 100  $\mu\text{L}$  of B16F10-luc-G5 tumor cells ( $1 \times 10^5$  in 100  $\mu\text{L}$ ) were injected subcutaneously into the right dorsal region near the thigh of the 20 Balb/C male mice using 1 mL syringe equipped with needle (size 25) after the mice had been anesthetized. The inoculation site was examined daily. When the tumor appeared, inoculated tumor growth was monitored by IVIS. After the mice had been anesthetized, 150 to 200  $\mu\text{L}$  of 15 mg/mL D-Luciferin were injected into their abdominal cavity in terms of the mice weight (10  $\mu\text{L}/\text{g}$ ). All mice were imaged individually at 15 min after luciferin injection under exposure conditions of 60 s, 10 bin, FOV 12.5, at day 0, 3, 5, 7 and 9. In order to correlate the intensities of bioluminescence to inoculated tumor size, 3 mice were executed at day 5 after IVIS detection for caliper measurement of the tumor. Tumor volumes (V) were obtained according to the formula:  $V=LW^2/2$ . The longest diameter (L) and maximum diameter (W) perpendicular to the direction of longest di-

ameter were measured by the vernier micrometer.

#### 1.5 Statistical Analysis

Statistical analysis was performed by analysis of correlation, followed by Chi-Square test and comparison between groups to detect statistically significant difference ( $P < 0.05$ ), using statistical software (SPSS, version 12.0).

## 2 RESULTS

### 2.1 Relationship between Bioluminescence and Number of Tumor Cells by IVIS

Table 1 clearly showed that the intensity of bioluminescence (the average number of measured photon) by IVIS was reduced while the number of B16F10-luc-G5 tumor cells was decreased from first 8th well, after exposed for 30 s, 60 s and 180 s respectively. The level and the scope of halo were also lowered (table 1). Taken 60 s as an example, as shown in fig. 1, the highest level and the largest scope of halo appeared in first well, followed by subsequently decrease in the remaining wells from second to 8th wells with the significant difference seen between the 7th and 8th wells. The measured average photon number had no significant difference between the groups when the exposure time was close, e.g. between the groups of 30 s and 60 s ( $P > 0.05$ ). However, there was no significant difference ( $P < 0.05$ ) among groups when the exposure time had a big gap, e.g. between the groups of 30 s and 180 s. A strong correlation between the number of tumor cells and the intensity of bioluminescence ( $R^2=0.99$ ) was also demonstrated under each exposure time. Formula and correlation coefficients ( $R^2$ ) were: 30 s,  $y=59.393x+560.03$ ,  $R^2=0.9982$ ; 60 s,  $y=60.69x+3892.8$ ,  $R^2=0.9981$ ; 180 s,  $y=66.59x+1125.9$ ,  $R^2=0.9979$ ; 360 s,  $y=74.97x+2908.2$ ,  $R^2=0.9979$ . The curves of 30 s and 60 s basically coincided with each other in fig. 2. It showed that both 30 s and 60 s were the optimal conditions for exposure because of the shortest exposure time, the largest  $R^2$  and basically coincided curves.

**Table 1 Correlation between the measured average photon and cell number under different exposure time (10 bin, FOV 12.5)**

Indexes	Well number								
	1 (A1)	2 (A5)	3 (A9)	4 (A12)	5 (E1)	6 (E5)	7 (E9)	8 (E12)	9 (H12)
Tumor cells number	$10^4$	$5 \times 10^3$	$2.5 \times 10^3$	$1.25 \times 10^3$	$6.25 \times 10^2$	$3.125 \times 10^2$	$1.56 \times 10^2$	$0.78 \times 10^2$	0
Average measured photon number in 30 s <sup>△</sup>	6.04E+05	2.81E+05	1.40E+05	8.00E+04	4.03E+04	2.33E+04	1.46E+04	4.50E+03	1.00E+03
Average measured photon number in 60 s <sup>△</sup>	6.21E+05	2.91E+05	1.44E+05	8.50E+04	4.20E+04	2.56E+04	1.86E+04	1.30E+04	1.22E+03
Average measured photon number in 180 s <sup>△</sup>	6.76E+05	3.23E+05	1.48E+05	9.60E+04	3.97E+04	2.41E+04	1.71E+04	1.17E+04	8.22E+03
Average measured photon number in 360 s <sup>△</sup>	7.99E+05	3.88E+05	1.71E+05	1.11E+05	4.21E+04	2.41E+04	1.69E+04	1.27E+04	1.12E+04

<sup>△</sup>:Units of photon number/( $\text{cm}^2 \cdot \text{sec} \cdot \text{s}$ ); H12 for blank control well

There was no significant difference in the average measured photon between the groups of 30 s and 60 s ( $P > 0.05$ ), but there was significant difference among the rest ( $P < 0.05$ ).

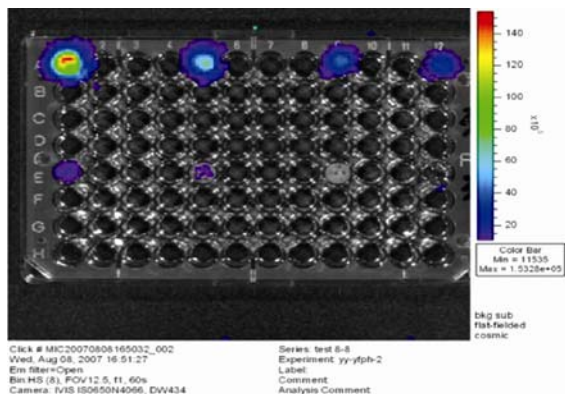


**Fig. 1** Relationship between bioluminescence and number of tumor cells by IVIS  
Line A were the well 1, 2, 3, 4 from left to right; Line E were the well 5, 6, 7, 8 from left to right

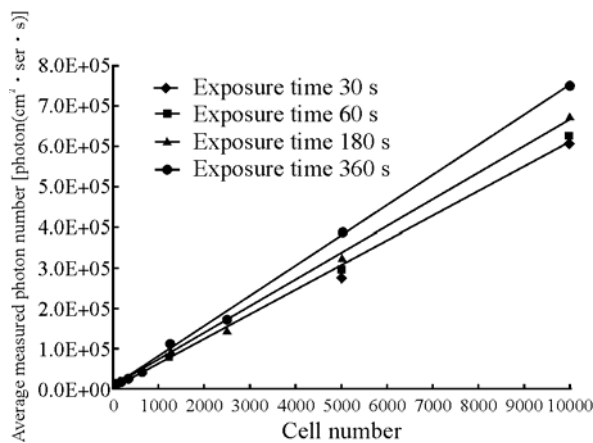


**Fig. 2** Correlation of average measured photon number and cell number under each exposure time  
Under each exposure time there was good correlation between the two indexes above, and the curves of 30 s and 60 s basically coincide with each other.

**2.2 Continuously Monitoring of Tumor Growth (Dynamic Morphology) by IVIS**

The size of tumor was too small to be examined visually or felt by touching on the day 0 to day 5 after inoculation. However, by using bioluminescence the tumors could be detected through day 0 to day 14 (table 2) even when it was invisible. There was significant difference in the bioluminescence of tumor cells (average measured photon number) from day 0 to day 9 ( $P<0.05$ ).

**Table 2 Bioluminescence and volume of inoculated tumor (exposure time: 60 s, 10 bin, FOV 12.5)**

Indexes	Different time points after transplantation					
	Day 0	Day 3	Day 5	Day 7	Day 9	Day 14
Average measured photon number <sup>△</sup>	(6.35E+05)±7655	(1.12E+05)±1820	(1.62E+05)±2090	(2.40E+05)±3515	(1.18E+06)±11530	(2.23E+06)±17934
Tumor volume (mm <sup>3</sup> )	--	--	(2.86E+00)±1.21	(4.87E+00)±1.66	(9.27E+01)±6.31	(2.60E+02)±7.88

<sup>△</sup>: Unit of photon number/(cm<sup>2</sup> · ser · s); Different time points after inoculation (Day 0 to Day 9); Comparison of the average photon number,  $P<0.01$ ; Day 0 and day 3: The tumor was too small to be measured visually.

Fig. 3 showed the correlation between the intensity of bioluminescence and the size of tumor on day 14.

**2.3 Bioluminescence of Inoculated Tumor Highly Correlated with Its Size**

The data of tumor volume on the day 5 after inoculation was shown in table 2, and a strong correlation ( $R^2=0.94$ ) between mean bioluminescence and mean tumor volume was demonstrated, with the formula and correlation coefficients:  $y=7939.3x+237606$ ,  $R^2=0.9791$  (fig. 4).

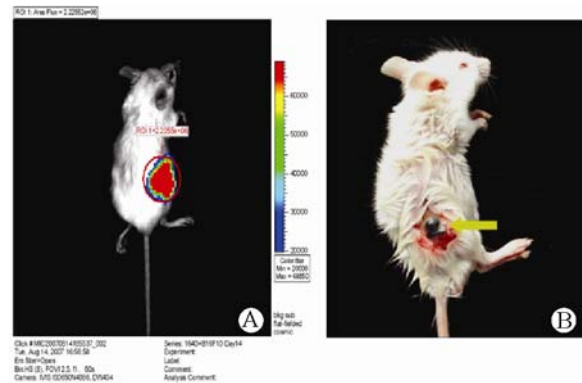


**Fig. 3** Bioluminescence and anatomical size of the same inoculated tumor (day 14)

Arrow showed the anatomical size of inoculated tumor.

A: Bioluminescence of inoculated tumor by IVIS (day 14); B: Anatomical size of inoculated tumor (day 14)

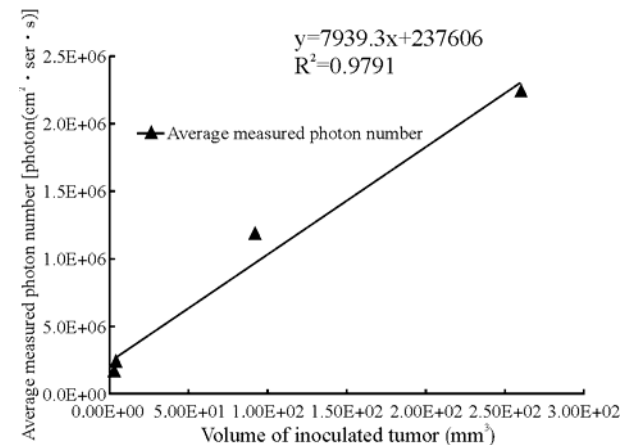


**Fig. 4** Correlation between bioluminescence and volume of inoculated tumor

There was a close correlation between the two indexes

### 3 DISCUSSION

Bioluminescence imaging detects light that is generated through the reaction of luciferase on its substrate, such as luciferin for firefly luciferase, in a living animal or cell samples. Bioluminescence process is virtually a chemical reaction between the luciferase and the substrate in the presence of adenosine 5'-triphosphate (ATP) and oxygen. Such chemical reaction excites the luminescent molecule and increases its energy level, resulting in fluorescence signals when it releases energy. The requirement of the presence of ATP makes bioluminescence signals only exist in the living cells<sup>[1]</sup>. To generate bioluminescence signals, the molecules, protein or cells of interest are labeled with optical probes, such as luciferase gene or green fluorescence gene. The optical probes then can be detected using a new and rapidly expanding technology known as optical molecular imaging to track and report their functional information<sup>[2]</sup>. IVIS is an instrument consisting of a very sensitive optical detection apparatuses, to detect bioluminescence or stimulate fluorescence signals with low-cost and non-invasiveness. IVIS has many advantages over other cell tracing methods, including higher sensitivity, less cells needed, constant marked signal (with optic reporter gene, constant gene of the genetically modified cells, light-emitting signal that is not weakened with the passage of cell division gradually), low noise level of imaging (except labeled cells, the other cells do not produce bioluminescence, therefore, the imaging of non-labeled cells can be ignored in background) and non-radioactivity. Moreover, the tracing system can still be cultivated and used continuously after the test, which saves cells and materials. In recent years, IVIS has been widely used to study oncology, virology, stem cells, transplantation immunology, protein and genetic research and many other fields<sup>[3-25]</sup>.

In addition to the above-mentioned advantages, another key but understudied advantage of IVIS is its capability to quantify the emitted light as a measurement of the reaction between luciferase and luciferin. Therefore, in this study, we specifically explored the quantitative analysis and the relevant methods of tracing cells by IVIS *in vitro* and *in vivo* systematically through the correlation analysis of the intensities of bioluminescence signals and number of cells. We used B16F10-luc-G5 cell line from the mouse melanoma cells, which were labeled with luciferase gene (luc). The luc gene is extracted from the North American's firefly (photinus pyralis), and can be expressed stably in all host cells producing a constant gene product—the luciferase<sup>[26]</sup>. As a result, the bioluminescence signals of cells will be saturated when light-emitting substrates are overdosed. B16F10-luc-G5 cell line was used for this study, because it has a moderate bioluminescence intensity and it is easy to be cultured (malignant cells). This study showed that, under each exposure time, bioluminescence by IVIS (measured average photon number) was highly relevant with cell number, and luminescence imaging indicated that bioluminescence signals were consistent with the level and the scope of halo. It is noted that the photon number in IVIS imaging is directly represented by the level and the scope of halo, so in the same color bar, the

more bias of level toward red, the greater the photon number would be, so as the scope of the corresponding halo.

Our *in vitro* assay results suggested that IVIS (bioluminescence measurement) could detect a very weak bioluminescence signal with high sensitivity. In this study, as few as 78 B16F10-luc-G5 cells could be detected with acceptable error by IVIS under the minimum exposure time of 30 s. Due to the intrinsic luminous characteristic of B16F10-luc-G5 cells, less than 78 cells under the same exposure time cannot be detected reliably. However, if cells have greater luminous intensity, they may be monitored with even fewer cells.

It is important to take into consideration factors that may affect the bioluminescence signal, such as exposure time. It was found that, under each exposure time, there was a linear regression relationship between the measured average photon number (y) and cell number (x), demonstrating that the cell number could be represented with bioluminescence (the photon number) from the cells. At 30 s and 60 s exposure time, there was no significant difference between the photon number and the same number of cells ( $P > 0.05$ ) (such as 30 s and 60 s). However, there was statistically significant difference in the average photon number detected under other different exposure conditions ( $P < 0.05$ ). Therefore, in order to quantify the bioluminescence signals as the number of labeled cells, it is required that the comparison is carried out under the same exposure condition.

Bioluminescence imaging is a highly sensitive molecular imaging modality, as it can detect and quantify cells transfected with the luciferase gene *in vivo*. We demonstrated the dynamics of the bioluminescence signals as a function of tumor size change. As *in vitro* assay, there was also a linear regression relationship between the bioluminescence signals and cell number *in vivo*. Therefore, we can trace the labeled cells (such as the growth state and migration path) through the detection of bioluminescence signals (quantitative amount of average photon and cell imaging).

In summary, we demonstrated a simple but accurate quantitative measurement of luciferase labeled cells both *in vitro* and *in vivo* using IVIS. The results may offer researchers a hint to explore the bioluminescence measurement to gain insight on the underlying biological processing by tracking and reporting functional information *in vitro* and *in vivo*.

### REFERENCES

- 1 Greer LF, Szalay AA. Imaging of light emission from the expression of luciferases in living cells and organisms: a review. *Luminescence*, 2002,17(1):43-74
- 2 Massoud TF, Gambhir SS. Molecular imaging in living subjects: seeing fundamental biological processes in a new light. *Genes Dev*, 2003,17(5):545-580
- 3 Larmonier N, Janikashvili N, LaCasse CJ, *et al.* Imatinib mesylate inhibits CD4+ CD25+ regulatory T cell activity and enhances active immunotherapy against BCR-ABL-tumors. *J Immunol*, 2008,181(10):6955-6963
- 4 Han Z, Fu A, Wang H, *et al.* Noninvasive assessment of cancer response to therapy. *Nat Med*, 2008,14(3):343-349
- 5 Xue W, Zender L, Miething C, *et al.* Senescence and tumour clearance is triggered by p53 restoration in murine

- liver carcinomas. *Nature*, 2007,445(7128):656-660
- 6 Tammela T, Saaristo A, Holopainen T, *et al.* Therapeutic differentiation and maturation of lymphatic vessels after lymph node dissection and transplantation. *Nat Med*, 2007,13(12):1458-1466
  - 7 Stephan MT, Ponomarev V, Brentjens RJ, *et al.* T cell-encoded CD80 and 4-1BBL induce auto- and transcostimulation, resulting in potent tumor rejection. *Nat Med*, 2007,13(12):1440-1449
  - 8 Dentin R, Liu Y, Koo SH, *et al.* Insulin modulates gluconeogenesis by inhibition of the coactivator TORC2. *Nature*, 2007,449(7160):366-369
  - 9 Zhang L, Lee KC, Bhojani MS, *et al.* Molecular imaging of Akt kinase activity. *Nat Med*, 2007,13(9):1114-1119
  - 10 Dierks C, Grbic J, Zirlik K, *et al.* Essential role of stromally induced hedgehog signaling in B-cell malignancies. *Nat Med*, 2007,13(8):944-951
  - 11 Barberi T, Bradbury M, Dincer Z, *et al.* Derivation of engraftable skeletal myoblasts from human embryonic stem cells. *Nat Med*, 2007,13(5):642-648
  - 12 Hajitou A, Rangel R, Trepel M, *et al.* Design and construction of targeted AAVP vectors for mammalian cell transduction. *Nat Prot*, 2007,2(3):523-531
  - 13 Murphy GJ, Mostoslavsky G, Kotton DN, *et al.* Exogenous control of mammalian gene expression via modulation of translational termination. *Nat Med*, 2006,12(9):1093-1099
  - 14 Zakrzewski JL, Kochman AA, Lu SX, *et al.* Adoptive transfer of T-cell precursors enhances T-cell reconstitution after allogeneic hematopoietic stem cell transplantation. *Nat Med*, 2006,12(9):1039-1047
  - 15 Negrin RS, Contag CH. *In vivo* imaging using bioluminescence: a tool for probing graft-versus-host disease. *Nat Rev*, 2006,6(6):484-490
  - 16 Franke-Fayard B, Waters AP, Janse CJ. Real-time *in vivo* imaging of transgenic bioluminescent blood stages of rodent malaria parasites in mice. *Nat Prot*, 2006,1(1):476-485
  - 17 Wehrman TS, von Degenfeld G, Krutzik PO, *et al.* Luminescent imaging of  $\beta$ -galactosidase activity in living subjects using sequential reporterenzymeluminescence. *Nat Methods*, 2006,3(4):295-301
  - 18 Thorne SH, Negrin RS, Contag CH. Synergistic antitumor effects of immune cell-viral biotherapy. *Science*, 2006,311:1780-1784
  - 19 Minn AJ, Gupta GP, Siegel PM, *et al.* Genes that mediate breast cancer metastasis to lung. *Nature*, 2005,436(28):518-524
  - 20 Morizono K, Xie Y, Ringpis GE, *et al.* Lentiviral retargeting to P-glycoprotein on metastatic melanoma through intravenous injection. *Nat Med*, 2005,11(3):346-352
  - 21 Kim JH, Kim B, Cai L, *et al.* Transcriptional regulation of a metastasis suppressor gene by Tip60 and  $\beta$ -catenin complexes. *Nature*, 2005,434(7035):921-926
  - 22 Hoebe K, Georgel P, Rutschmann S, *et al.* CD36 is a sensor of diacylglycerides. *Nature*, 2005,433(7025):523-527
  - 23 Bins AD, Jorritsma A, Wolkers MC, *et al.* A rapid and potent DNA vaccination strategy defined by *in vivo* monitoring of antigen expression. *Nat Med*, 2005,11(8):899
  - 24 Gross S, Piwnica-Worms D. Real-time imaging of ligand-induced IKK activation in intact cells and in living mice. *Nat Methods*, 2005,2(8):607-614
  - 25 Levenberg S, Rouwkema J, Macdonald M, *et al.* Engineering vascularized skeletal muscle tissue. *Nat Biotechnol*, 2005,23(7):879-884
  - 26 Greer LF, Szalay AA. Imaging of light emission from the expression of luciferases in living cells and organisms: a review. *Luminescence*, 2002,17(1):43-74

(Received Nov. 23, 2009)